ACS EARTH AND SPACE CHEMISTRY

http://pubs.acs.org/journal/aesccq

Article

Oxidation of Dipropyl Thiosulfinate Initiated by Cl Radicals in the Gas Phase: Implications for Atmospheric Chemistry

Parandaman Arathala and Rabi A. Musah*

Cite This: *ACS Earth Space Chem.* 2021, 5, 2878−2890

Read Online

ACCESS | Metrics & More | Article Recommendations | Supporting Information

ABSTRACT: The reaction mechanism for chlorine radical (•Cl)-initiated atmospheric oxidation of dipropyl thiosulfinate (DPTS) in the gas phase was investigated using ab initio/density functional theory electronic structure calculations. The DPTS + •Cl reaction proceeds by H-abstraction and substitution pathways. The results indicate that the Cl radical adds to the S-atom of the sulfinyl [S(═O)] group of DPTS, which is followed by cleavage of the S(═O)−S single bond, leading to the formation of propanesulfinyl chloride and propanethiyl radical (PTR). The barrier height for this reaction was estimated to be −12.2 kcal mol^{-1} relative to the separated starting reactants. The rate coefficients were calculated for all possible H-abstraction and substitution paths using the master equation solver for the multi-energy well reactions (MESMER) kinetic code in the atmospherically relevant temperature range of 200−300 K and at 1 atm pressure. The rate coefficient data for all reaction paths indicate that the formation of propanesulfinyl chloride and PTR from the DPTS + •Cl reaction is the major path. The rate coefficient for this reaction was estimated to be ∼6.00 × 10^{-10} cm^3 molecule^{-1} s^{-1} at 298 K and 1 atm pressure. The overall rate coefficient for the DPTS + •Cl reaction in the same temperature range was found to be ∼8.14 × 10^{-10} cm^3 molecule^{-1} s^{-1} at 298 K. The atmospheric lifetime of DPTS was calculated to be ∼3 h in the temperatures between 200 and 300 K and at 1 atm. In addition, the branching ratio fractions for each reaction were determined and the atmospheric implications are discussed. Overall, the results reveal that while the primary products of the DPTS + Cl radical reaction are short-lived, the compounds formed from their subsequent oxidative degradation do contribute to global warming and have the potential to exhibit adverse environmental impacts.

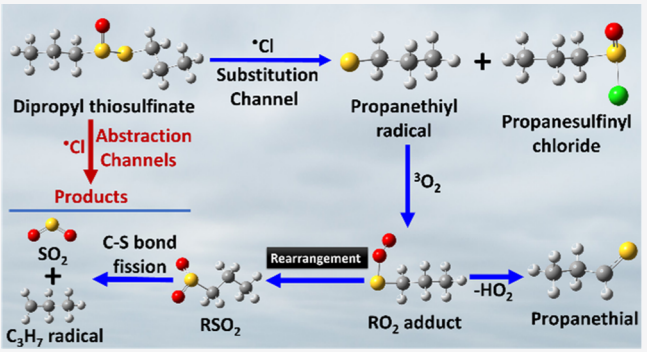

KEYWORDS: *dipropyl thiosulfinate, Cl radical, barrier height, rate coefficient, branching ratio, atmospheric lifetime, propanesulfinyl chloride*

1. INTRODUCTION

A broad range of volatile organosulfur compounds (VOSCs) are known to be released into the atmosphere from various natural and anthropogenic sources.[1] The contribution to the atmospheric sulfur budget of biogenically derived VOSCs is estimated to be as high as 50%.[2] As such, natural source VOSCs may have a major impact on the global sulfur cycle. S-containing compounds such as hydrogen sulfide (H_2S), methane thiol (CH_3SH), and dimethyl sulfide [(DMS), $(CH_3)_2S$] are known to play a crucial role in tropospheric chemistry as their atmospheric oxidation can lead to the formation of acid rain and climate change.[3,4] Regardless of their source, VOSCs in the atmosphere can undergo degradation through photolysis and/or reaction with several oxidants [e.g., •OH, •Cl, NO_x, and ozone (O_3)], leading to their removal or conversion into other compounds which themselves serve as atmospheric pollutants.[5−8] Thus, the emitted VOSCs and their oxidation products contribute to global warming, acid precipitation, cloud formation, and the formation of secondary organic aerosols (SOAs).[9]

Dipropyl thiosulfinate (DPTS) is an example of an important plant-derived trace compound. It is emitted from onion, garlic, shallot, and other similar *Allium* genus cash crops that occupy large acreage on farmlands.[10] Because of the prevalence of OH radicals in the troposphere,[11] it is anticipated that the process of removal of DPTS from the atmosphere may involve its reactions with this radical.[12] A recent computational study indicated that the DPTS + •OH reaction is relatively fast and appears to be the most dominant gas phase atmospheric removal process for this compound.[11] The DPTS + •OH reaction mainly proceeds

Received: July 6, 2021
Revised: August 12, 2021
Accepted: August 15, 2021
Published: September 3, 2021

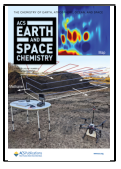

https://doi.org/10.1021/acsearthspacechem.1c00246
ACS Earth Space Chem. 2021, 5, 2878−2890

Scheme 1. DPTS + •Cl Reaction Mechanism Involving H-Atom Abstraction Pathways (Indicated by Red Arrows), Leading to the Formation of HCl and Various C-Centered Radical Products; and Substitution Pathways (Indicated by Blue Arrows) Leading to the Formation of Various Chlorinated Organosulfur Compounds

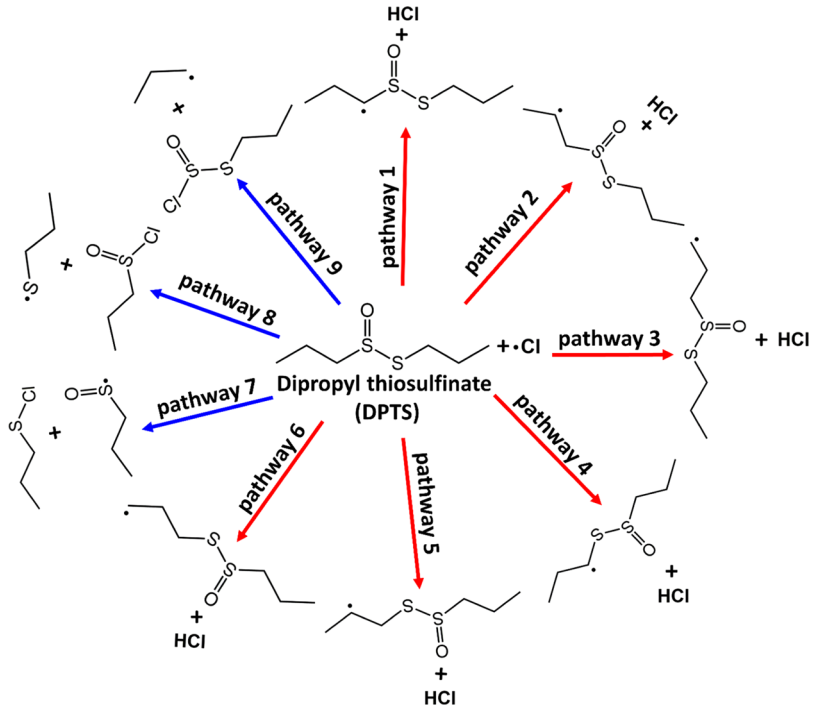

through addition of •OH to the S-atom of the sulfinyl [S(═O)] group followed by S−S(═O) single bond cleavage, leading to the formation of propanesulfinic acid (PSIA) and propanethiyl radical (PTR). The rate coefficient for this reaction was reported to be 1.7×10^{-10} cm^3 $molecule^{-1}$ s^{-1} at 300 K, which corresponds to an atmospheric lifetime of DPTS with respect to its reaction with OH radical of less than 2 h. The atmospheric oxidation of the related compound dimethyl thiosulfinate (DMTS) initiated by OH/Cl radicals has also been reported.[13] The reaction mechanism of DMTS with •OH/•Cl suggests that similar to the reaction path observed for DPTS + •OH, addition of an •OH/•Cl to the S-atom of the −S(═O) group occurs. This is followed by S−S(═O) single bond fission, leading to the formation of methanethiyl radical + methanesulfinic acid and methanethiyl radical + methanesulfinyl chloride, for •OH and •Cl, respectively. The rate coefficients for the DMTS + •OH and DMTS + •Cl reactions were found to be 1.42×10^{-11} and 3.72×10^{-11} cm^3 $molecule^{-1}$ s^{-1} at 300 K. The corresponding atmospheric lifetimes of DMTS with respect to •OH and •Cl at 298 K were reported to be 0.8 and 2.4 days, respectively. Based on the results of the DPTS + •OH and DMTS + •OH/•Cl studies, the atmospheric removal of these VOSCs is mostly due to the reactions with OH and Cl radicals, although the reactions involving the OH radical are more dominant. The importance of the Cl radical reactions is mainly due to the significant concentrations of Cl radicals that are present over the marine boundary layer.[14−16] While ozone (O_3) is another oxidizing species present in the atmosphere of the marine boundary layer, its reactions with VOSCs are quite slow compared with those of OH and Cl radicals.[7] To reveal a more complete picture regarding the environmental fate and impact of the plant-derived thiosulfinate congener series, an understanding of the reactions of DPTS with Cl radical is required.

To date, there are no reports of experimental or theoretical studies of the atmospheric oxidation of DPTS via its interaction with •Cl. Therefore, we investigated the oxidation mechanism and energies of the gas phase DPTS + •Cl reaction using quantum chemistry calculations. The results revealed that the mechanism proceeds primarily through H-abstraction pathways due to the presence of the hydrogen atoms associated with the methyl ($-CH_3$) and methylene ($-CH_2-$) moieties of DPTS. It was also observed that the DPTS + •Cl reaction can proceed by substitution pathways through addition of a Cl radical to the S-atom of the sulfinyl [S(═O)] or S-atom sites of DPTS, followed by cleavage of either the S(═O)−S or S(═O)−C single bond, respectively, leading to the formation of various reaction products (as illustrated in Scheme 1, pathways 1−9). In Scheme 1, reactions 1−6 represent paths where abstraction of an H-atom from the $-CH_2$ or $-CH_3$ groups of DPTS by the Cl radical leads to the formation of various C-centered radical products along with molecular hydrochloric acid (HCl). The remaining reactions (pathways 7−9) represent the substitutions that lead to the formation of the corresponding chlorinated organosulfur compounds.

Several previously reported experimental and theoretical studies indicate that the oxidation of various VOSCs in the presence of atmospheric oxidants such as OH and Cl radicals each proceed via formation of a weakly bound complex.[5,17−20] These complexes are formed by addition of the radical oxidant (OH or Cl) to the S-atom of the VOSCs which results in the formation of two-center three electron (2c−3e) bonds. Experimental evidence for the formation of such complexes with DMS and dimethyl sulfoxide (DMSO), that is, the OH−DMS, Cl−DMS, and Cl−DMSO complexes, has been reported.[5,17,19,20] These studies also suggest that complex formation may play a key role in the oxidation of VOSCs in the atmosphere. The results of theoretical studies of the

https://doi.org/10.1021/acsearthspacechem.1c00246
ACS Earth Space Chem. 2021, 5, 2878−2890

reactions of H_2S, DMS, and DMTS with OH and Cl radicals also support the formation of complexes through 2c−3e bonds. These stable complexes may influence the reaction rates and thereby the atmospheric fate of the compounds.[13,21,22]

In the present work, we conducted a theoretical study of the oxidation of DPTS with Cl radicals to gain greater insights into the oxidation process. Density functional and ab initio calculations were performed to reveal the reaction mechanism, energetics, and kinetics of all the possible pathways associated with the DPTS + $^{\bullet}$Cl reaction (see Scheme 1). In addition, rate coefficients for reaction pathways 1−9 were calculated using the potential energy surfaces (PESs) determined from the quantum calculations, and these were used in the master equation solver for the multi-energy well reaction (MESMER)[23] kinetic code in the temperature range of 200−300 K and at 1 atm pressure. The details of the reaction mechanism, energies of the key stationary points on the PESs for all reaction paths, the rate coefficients, branching ratios, and atmospheric implications are discussed. The results contribute to our understanding of the tropospheric chemistry of DPTS in the presence of Cl radicals and the formation of various reaction products as atmospheric pollutants.

2. COMPUTATIONAL METHODS

All of the key stationary point molecular geometries on the PESs for the H-abstraction and substitution paths associated with the DPTS + $^{\bullet}$Cl reaction were optimized using the M06-2X[24] hybrid density functional with an augmented correlation-consistent polarized valence triple zeta (aug-cc-pVTZ) basis set.[25] Previous studies on the oxidation of various alkylthiosulfinates and other sulfur compounds initiated by $^{\bullet}$OH and $^{\bullet}$Cl indicate that the M06-2X functional performs well for determination of the reaction mechanism, rate coefficients, and thermochemistry.[11,13,26] The harmonic vibrational frequencies were calculated using the same computational level for all the optimized geometries to confirm the nature of the stationary points. Various minima on the PESs such as isolated reactants, pre-reactive complexes (RCs), post-reactive complexes (PCs), and products were all identified with positive vibrational frequencies, and all the transition states (TSs) were identified with one negative frequency. Intrinsic reaction coordinate calculations[27,28] for all the TSs were performed using the same M06-2X/aug-cc-pVTZ level of theory to confirm that each TS was connected to the corresponding RC and PC structures in the reaction. To improve the energies for all molecular species involved in the DPTS + $^{\bullet}$Cl reaction paths, single-point energy calculations were performed at the CCSD(T)/cc-pVTZ level.[29] In this work, the Gaussian 16 program suite[30] was used to perform all the electronic structure calculations. The energies reported for all the key stationary points on the PESs were calculated at the CCSD(T)/cc-pVTZ//M06-2X/aug-cc-pVTZ (defined as CCSD(T)//M06-2X) level, with zero-point energy (ZPE) corrections carried out at the M06-2X/aug-cc-pVTZ level. The S-atoms in DPTS are in the singlet state. Dissociation of the reactant in the presence of the Cl radical leads to the formation of radical and molecular products. The spin states of the radical and molecule products are doublet and singlet, respectively. We also calculated T1 diagnostic values for all the stationary points to verify the reliability of the results using a single reference wave function, and the values are presented in Table S1 of the Supporting Information. This was carried out because previous reports[31] suggest that T1 values above 0.02 for any stationary point species are somewhat less reliable and should be treated with multireference methods. The T1 values for all the species in this work were found to be below 0.02 (see Table S1). This observation indicates that the reported calculations can be expected to yield reliable results for the reaction energetics.

3. RESULTS AND DISCUSSION

The stable conformer of DPTS reported in our previous work and which was computed at the M06-2X/6-311++G(3df,3pd) level[11] was used to perform the calculations described herein by reoptimizing the same structure at the M06-2X/aug-cc-pVTZ level. The resultant optimized geometry of DPTS was used as a starting reactant (see Figure 1). The energy of DPTS calculated

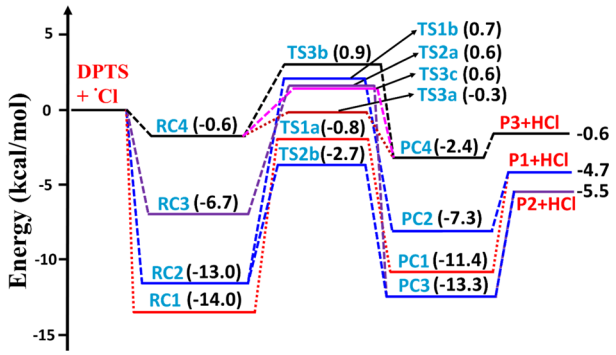

Figure 1. PES diagram for the abstraction of the hydrogen atom by the Cl radical from the $CH_3-CH_2-CH_2-S(=O)-$ group of DPTS obtained at the CCSD(T)/cc-pVTZ//M06-2X/aug-cc-pVTZ level. The symbols are defined as follows: RC1−RC4 (pre-reactive complexes); TS*N*a, TS*N*b, and TS*N*c (*N* = 1−3; transition states); PC1−PC4 (post-reactive complexes); and P1−P3 (C-atom centered DPTS radical products).

at the CCSD(T)/cc-pVTZ//M06-2X/aug-cc-pVTZ level in the present work differed from the previously reported value that was computed at the CCSD(T)/cc-pVTZ//M06-2X/6-311++G(3df,3pd) level[11] by ∼0.2 kcal mol^{-1}. This suggests that the calculations carried out at the CCSD(T)/cc-pVTZ//M06-2X/aug-cc-pVTZ level predict reasonably good energies. The DPTS + $^{\bullet}$Cl reaction mainly proceeds through H-abstraction (pathways 1−6) and substitution (pathways 7−9), as shown in Scheme 1. The H-atom abstraction from the various $-CH_2$ and $-CH_3$ sites of DPTS by the Cl radical occurs to form the indicated radical products (pathways 1−6 in Scheme 1). Pathway 7 represents a mechanism that proceeds via addition of the Cl radical to the S-atom followed by cleavage of the S(=O)−S single bond, leading to the formation of propanesulfenyl chloride ($CH_3CH_2CH_2SCl$) and propylsulfinyl radical [$CH_3CH_2CH_2S^{\bullet}(=O)$]. The other two remaining pathways (i.e., 8 and 9) represent the addition of the Cl radical to the sulfinyl S-atom followed by cleavage of the S(=O)−S or S(=O)−C single bonds, leading to the formation of propanesulfinyl chloride ($CH_3CH_2CH_2S(O)Cl$) + PTR ($CH_3CH_2CH_2S^{\bullet}$), and $CH_3CH_2CH_2SS(O)Cl$ + propyl radical ($CH_3CH_2C^{\bullet}H_2$), respectively.

To learn more about the relative importance of each of the paths 1 through 9, the branching ratio contributions of the various paths, and the distribution of final products, electronic structure calculations were carried out for all passible DPTS + Cl radical reaction paths by exploring the stationary point geometries on the PESs. For each reaction path 1−9, the corresponding RC, PC, TS, and products were characterized by

https://doi.org/10.1021/acsearthspacechem.1c00246
ACS Earth Space Chem. 2021, 5, 2878−2890

vibrational frequency calculations. The energies of all the stationary points on the PESs were calculated at the CCSD(T)/cc-pVTZ//M06-2X/aug-cc-pVTZ level. The total electronic energies (E_{total}) along with the ZPE-corrected electronic energies [E_{total}(ZPE)] of the reactants, RCs, PCs, TSs, and products obtained at the M06-2X/aug-cc-pVTZ and CCSD(T)/cc-pVTZ levels are given in Table S2. The ZPE at the M06-2X/aug-cc-pVTZ level was used to correct the single-point energy obtained at the CCSD(T)/cc-pVTZ level to get the ZPE-corrected electronic energies [E_{total}(ZPE)] for all the stationary points. The imaginary frequencies of the various TSs, rotational constants, vibrational frequencies, and optimized geometries of all the stationary points obtained at the M06-2X/aug-cc-pVTZ level are provided in Tables S3−S6 of the Supporting Information.

3.1. Stationary Points on the PES and Barrier Heights.

3.1.1. Abstraction Channels. As a consequence of the presence of two distinct propyl groups in DPTS (i.e., one attached to the sulfinyl [−S(=O)] group and the other to the S-atom), there are 14 unique H-atoms attached to carbon that can be abstracted via 14 different TSs. The TSs for each H-abstraction pathway associated with the DPTS + $^{\bullet}$Cl reaction, as indicated in Scheme 1, are labeled TS1a and TS1b for pathway 1; TS2a and TS2b for pathway 2; TS3a, TS3b, and TS3c for pathway 3; TS4a and TS4b for pathway 4; TS5a and TS5b for pathway 5; and TS6a, TS6b, and TS6c for pathway 6. The labeling of each H-abstraction TS in the structure of DPTS is illustrated below.

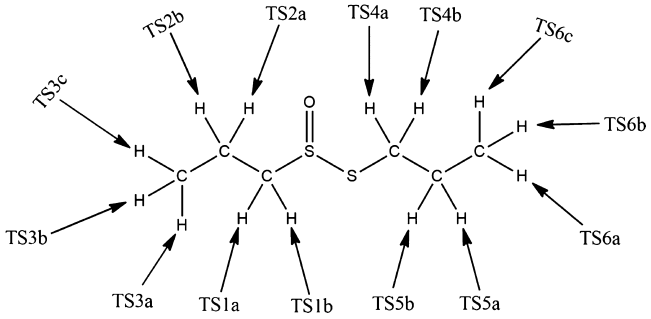

Also, the C-centered DPTS radical products formed from each H-abstraction path (1−6) are labeled Pn (n = 1−6) with a molecular hydrochloric acid (HCl). Similarly, the TSs for the substitution pathways are labeled TS7a and TS7b for pathway 7; TS8 for pathway 8; and TS9 for pathway 9, respectively. The corresponding substitution pathway products are labeled P7a and P7b for pathway 7; P8a and P8b for pathway 8; and P9a and P9b for pathway 9.

The PES profiles for abstraction of the H-atoms from the propyl moiety attached to the S-atom of the sulfinyl [−S(=O)] moiety of DPTS are shown in Figure 1. The stationary point energies were calculated relative to the starting separated reactants (DPTS + $^{\bullet}$Cl), and the corresponding energies that are displayed in the figure were calculated at the ZPE-corrected CCSD(T)//M06-2X level. The geometries and structural parameters of all the TSs optimized at the M06-2X/aug-cc-pVTZ level are shown in Figure 2, and the geometries and structural parameters of the RCs and PCs optimized at the same level are shown in Figure S1 of the Supporting Information The PES profiles, as shown in Figure 1, indicate that each of the H-atom abstraction paths involved in the DPTS and $^{\bullet}$Cl reactions primarily undergoes association to form RCs such as RC1, RC2, RC3, and RC4 with corresponding binding energies of 14.0, 13.0, 6.7, and 0.6 kcal mol^{-1} below that of the starting reactants, respectively. The formed RC1 proceeds to the formation of PC1 with an energy of −11.4 kcal mol^{-1} on the PES through a TS (TS1a) with a barrier height of −0.8 kcal mol^{-1} relative to the starting reactants. The structures of RC1 and TS1a from Figures S1 and 2 suggest that the movement of the Cl radical occurs in such a way that it abstracts the H-atom from the methylene group directly attached to the −S(=O) moiety of DPTS. The reaction then proceeds further via unimolecular dissociation of PC1 to form the corresponding bimolecular separated products [P1 ($CH_3CH_2C^{\bullet}H-S(O)-S-CH_2CH_2CH_3$) + H_2O] with an energy of ∼−4.7 kcal mol^{-1} below that of the reactants. The RC2 proceeds through the formation of two different TSs (TS1b and TS2b) with barrier heights of ∼0.7 and −2.7 kcal mol^{-1} above and below the starting reactants, respectively. These two reactions then lead to the corresponding PCs (PC2, and PC3) with energies of −7.3 and −13.3 kcal mol^{-1}, respectively. PC2 further proceeds to the formation of P1 [$CH_3CH_2C^{\bullet}H-S(O)-S-CH_2CH_2CH_3$ + HCl]. The other formed PC3 undergoes decomposition to form P2 [$CH_3C^{\bullet}HCH_2-S(O)-S-CH_2CH_2CH_3$ + HCl] as products at −5.5 kcal mol^{-1} on the PES (see Figure 1). RC3 from the association of DPTS and Cl radical proceeds to form a TS (TS2a) with a barrier height of ∼0.6 kcal mol^{-1} above the starting reactants, which continues first to form PC3 and then to form P2 [$CH_3C^{\bullet}HCH_2-S(O)-S-CH_2CH_2CH_3$ + HCl] as final products. The RC4 also undergoes three different H-abstraction paths via TSs (TS3a, TS3b, and TS3c) with barrier heights of −0.3, 0.9, and 0.6 kcal mol^{-1} relative to the starting reactants, respectively. These three TSs then lead to the formation of the same PC4 with an energy of ∼−0.6 kcal mol^{-1}, which then leads to the formation of products [P3 ($C^{\bullet}H_2CH_2CH_2-S(O)-S-CH_2CH_2CH_3$) + HCl]. Based on the PESs, as shown in Figure 1, it can be concluded that abstraction by the Cl radical of an H-atom from the center C-atom of the propyl moiety that is attached to the sulfinyl group of DPTS, and which proceeds first through RC2 to form TS2b, and then to form PC3 and the corresponding products [P2 ($CH_3C^{\bullet}HCH_2-S(O)-S-CH_2CH_2CH_3$) + HCl] is the dominant reaction when compared to all other possible H-abstractions from the propyl group attached to the sulfinyl S-atom of DPTS.

The calculations for abstraction by Cl radicals of H-atoms from the propyl group attached to the S-atom of DPTS were performed using the same level of theory. The PES profiles involving all the key stationary points calculated at the ZPE-corrected CCSD(T)//M06-2X level are shown in Figure 3, and the corresponding optimized geometries and structural parameters of all the species obtained at the M06-2X/aug-cc-pVTZ level are shown in Figures 2 and S1 of the Supporting Information. The data from the PESs suggest that Cl initiated H-atom abstraction paths involving DPTS lead to the formation of RC1, RC3, and RC5. These complexes can be seen at the entrance channels of the PESs with binding energies of 14.0, 6.7, and 17.1 kcal mol^{-1} below that of the starting reactants. The RC1 proceeds to form a TS (TS4b) with a barrier height of −2.8 kcal mol^{-1} relative to the energy of the starting DPTS + $^{\bullet}$Cl separated reactants. This reaction advances further to form the corresponding products $CH_3CH_2CH_2S(O)SC^{\bullet}HCH_2CH_3$ (P4) + HCl with an energy of −6.5 kcal mol^{-1} on the PES, through the decomposition of PC5 located at −15.3 kcal mol^{-1}. RC3 proceeds through two different H-atom abstraction channels by forming two different TSs (TS4a and TS6c) with barrier heights of −0.6 and 0.8 kcal mol^{-1} below and above the starting reactants, respectively. The formed TSs lead to the

https://doi.org/10.1021/acsearthspacechem.1c00246
ACS Earth Space Chem. 2021, 5, 2878−2890

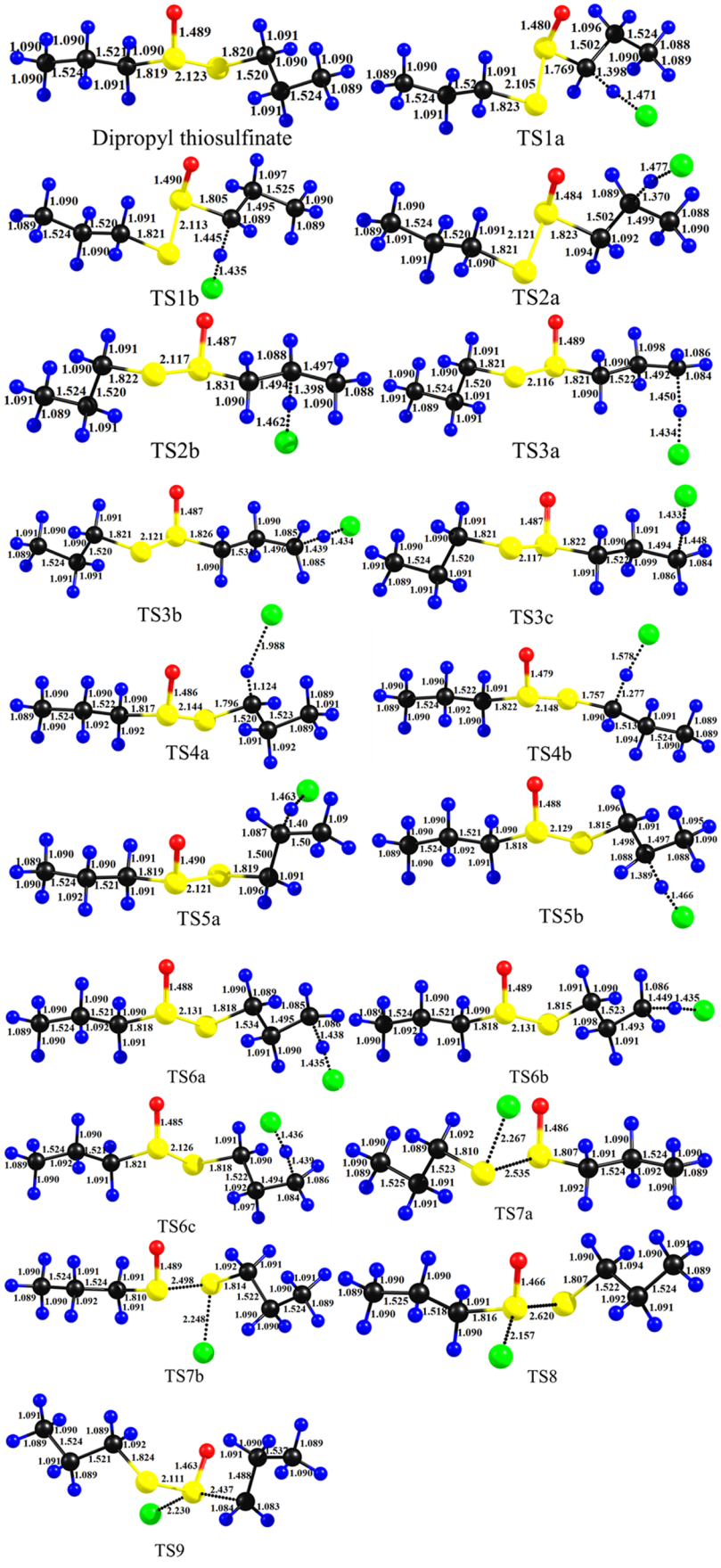

Figure 2. M06-2X/aug-cc-pVTZ level-optimized molecular geometries of the reactant DPTS and all possible TSs associated with its reaction with $^{\bullet}$Cl. The black, yellow, red, green, and blue colors represent carbon, sulfur, oxygen, chlorine, and hydrogen atoms, respectively. The bond lengths (Å) provided on the structures were obtained at the M06-2X/aug-cc-pVTZ level.

https://doi.org/10.1021/acsearthspacechem.1c00246
ACS Earth Space Chem. 2021, 5, 2878−2890

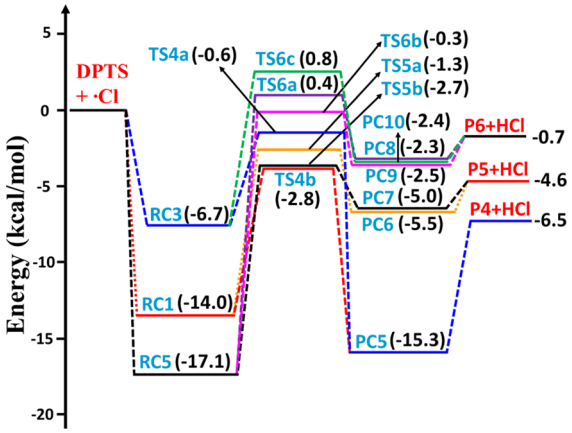

Figure 3. PES diagram for the abstraction of the hydrogen atom by the Cl radical from the $CH_3-CH_2-CH_2-S-$ group of DPTS obtained at the CCSD(T)/cc-pVTZ//M06-2X/aug-cc-pVTZ level. The symbols are defined as follows: RC1, RC3, and RC5 (pre-reactive complexes); TS*N*a, TS*N*b and TS*N*c (*N* = 4−6; transition states); PC5−PC10 (post-reactive complexes); and P4−P6 (C-atom centered DPTS radical products).

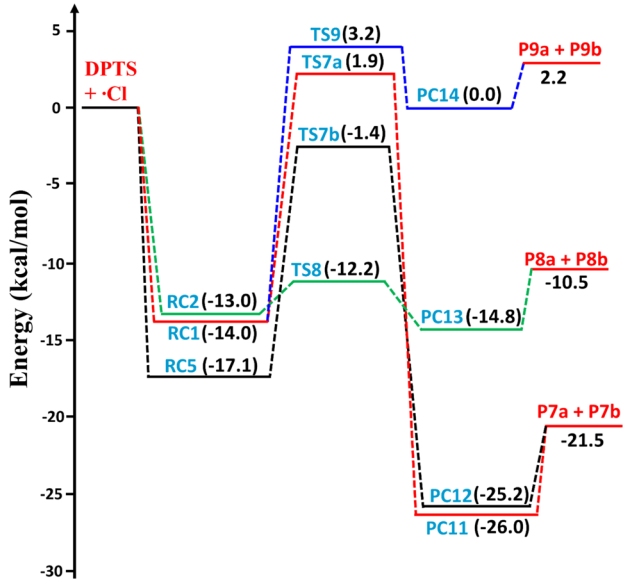

Figure 4. PES diagram for the various substitution channels involved in the DPTS + •Cl → products obtained at the CCSD(T)/cc-pVTZ//M06-2X/aug-cc-pVTZ level. The symbols are defined as follows: RC1, RC2, and RC5 (pre-reactive complexes); TS7a, TS7b, TS8 and TS9 (transition states); PC11−PC14 (post-reactive complexes); and P*N*a−P*N*b (*N* = 7−9; products).

corresponding PCs (PC5 and PC10) with energies of −15.3 and −2.4 kcal mol^{-1} below the reactants. These PCs lead to the formation of the corresponding final products $CH_3CH_2CH_2S(O)SC^{\bullet}HCH_2CH_3$ (P4) + HCl and $CH_3CH_2CH_2S(O)SCH_2CH_2C^{\bullet}H_2$ (P6) + HCl with corresponding energies of −6.5 and −0.7 kcal mol^{-1}, respectively. The remaining RC5 also proceeds through four different H-atom abstraction channels via the formation of four different TSs (TS5a, TS5b, TS6a, and TS6b) with barrier heights of −1.3, −2.7, 0.4, and −0.3 kcal mol^{-1} relative to the starting reactants, respectively. These four abstraction reactions continue to form the corresponding PCs (PC6, PC7, PC8, and PC9) with energies of −5.5, −5.0, −2.3 and −2.5 kcal mol^{-1}, respectively. These PCs dissociate to form the corresponding products $[CH_3CH_2CH_2S(O)SCH_2C^{\bullet}HCH_3$ (P5) + HCl and $CH_3CH_2CH_2S(O)SCH_2CH_2C^{\bullet}H_2$ (P6) + HCl]. The PES profile for the Cl radical-initiated H-atom abstraction from the propyl group attached to the S-atom of DPTS through TS4b with a barrier height of −2.8 kcal mol^{-1}, was found to be energetically more feasible in comparison to the other possible H-atom abstraction paths, as illustrated in Figure 3.

3.1.2. Substitution Channels. Besides Cl radical-initiated abstraction, a number of substitution reaction channels are available for the DPTS + •Cl reaction. These are presented as pathways 7−9 in Scheme 1, and they lead to the formation of the indicated substitution products. We investigated the energetics of these possible reactions using the computational approach described above for the investigation of the abstraction pathways. The PES profiles involving all the stationary points for these reactions are shown in Figure 4, and the optimized geometries obtained at the M06-2X/aug-cc-pVTZ level are shown in Figure 2 and Figure S1 of the Supporting Information. The ZPE-corrected CCSD(T)//M06-2X level calculated energies of all the stationary points relative to the starting reactants are displayed in Figure 4. Similar to the abstraction channels, association of DPTS and Cl radical leads to the formation of a barrierless RC1 with a binding energy of ∼14.0 kcal mol^{-1} below that of the starting reactants. This reaction proceeds to a TS (TS7a) with a barrier height of 1.9 kcal mol^{-1} above the starting reactants (see Figure 4). Its structure shown in Figure 2 suggests that the Cl radical attacks above the plane of the S-atom of DPTS and forms a single bond to the S-atom, and that this step occurs concomitantly with cleavage of the S(=O)−S single bond of DPTS. The simultaneous cleavage of the S(=O)−S single bond and formation of the S−Cl single bond in the TS structure is illustrated by the dashed lines between the atoms in Figure 2. TS7a leads to the formation of PC11 with a stabilization energy of ∼26.0 kcal mol^{-1} below that of the starting reactants. Finally, products $CH_3CH_2CH_2S^{\bullet}(O)$ (P7a) + $CH_3CH_2CH_2SCl$ (P7b) are formed from the unimolecular decomposition of PC11. Interestingly, we found an alternative TS for the formation of the same two products (i.e., P7a and P7b). In this reaction, DPTS and •Cl initially form a more stable RC5 with an energy of ∼−17.1 kcal mol^{-1} which leads to the formation of a TS (TS7b) with a barrier height of ∼−1.4 kcal mol^{-1} relative to that of the starting reactants. The structure of TS7b indicates that the Cl radical attacks from below the plane of the S-atom of DPTS, and this is followed by cleavage of the S(=O)−S single bond (see Figure 2). TS7b then proceeds first to form PC12 and then to the final products P7a $[CH_3CH_2CH_2S^{\bullet}(O)]$ and P7b ($CH_3CH_2CH_2SCl$).

The other possible substitution channels include Cl radical attack on the S-atom of the sulfinyl group [−S(=O)] in DPTS followed by cleavage of the S−S(=O) single bond, leading to the formation of $CH_3CH_2CH_2S(O)-Cl$ (P8a) + $CH_3CH_2CH_2S^{\bullet}$ (P8b). This pathway starts from the interaction of DPTS + •Cl as separated reactants to form RC2 which then proceeds to form a TS (TS8) with a barrier height of −12.2 kcal mol^{-1} relative to that of the starting reactant. The structure of TS8 (see Figure 2) suggests that addition of the Cl radical occurs at the sulfinyl S-atom to form a new S(=O)−Cl single bond, and this is followed by cleavage of the S(=O)−S single bond. TS8 leads to the formation of PC13 with an energy of −14.8 kcal mol^{-1} relative to that of the starting reactants. This then proceeds to the formation of P8a ($CH_3CH_2CH_2S(O)-Cl$) + P8b ($CH_3CH_2CH_2S^{\bullet}$) with an energy of −10.5 kcal mol^{-1} (see

https://doi.org/10.1021/acsearthspacechem.1c00246
ACS Earth Space Chem. 2021, 5, 2878−2890

Figure 4). In the course of these studies, we also found one additional substitution channel whose TS structure (TS9) indicates that the Cl radical added to the S-atom of the sulfinyl moiety, forming a new S(=O)−Cl bond. This step is then followed by dissociation of the S(=O)−C single bond. This reaction path also starts from the separated reactants (DPTS + Cl), which then undergo formation of a TS (TS9) between RC2 and PC14 with a barrier height of ∼3.2 kcal mol^{-1} above that of the separated reactants. PC14 proceeds to form $CH_3CH_2CH_2SS(O)-Cl$ (P9a) + propyl radical [$CH_3CH_2C^{\bullet}H_2$, (P9b)] as final products. Based on the PES profiles, as shown in Figures 1, 3, and 4, it is concluded that Cl radical addition to the S-atom of the sulfinyl group [S(=O)] followed by dissociation of the S−S(=O) single bond through TS (TS8), leading to the formation of $CH_3CH_2CH_2S(O)-Cl$ (P8a) + $CH_3CH_2CH_2S^{\bullet}$ (P8b) as final products, is the most energetically feasible reaction when compared to all possible H-abstraction and substitution paths available to the DPTS + $^{\bullet}$Cl reaction system.

In our studies of the DPTS + $^{\bullet}$Cl reaction mechanism, RCs such as RC1, RC2, and RC5 were found to be more stable with binding energies of 14.0, 13.0, and 17.1 kcal mol^{-1} relative to the energies of the starting reactants (see Figures 1, 3, and 4). The main reason for their greater stability is that they form 2-center−3-electron (2c−3e) bonds between the lone pair electrons of the sulfur atom of DPTS and the single electron occupied p-orbital of the Cl radical. This interaction, as represented with a dashed line with a bond length of r_{S-Cl} = 2.55 Å, is readily apparent in the RCs (RC1, RC2, and RC5), as shown in Figure S1 of the Supporting Information. The 2c−3e bonds in the various complexes have been reported in previous studies involving the interaction of various sulfur and nitrogen containing compounds with Cl radicals.[13,32−35] The paths involving the DPTS + $^{\bullet}$Cl reaction also form 2c−3e bond complexes through weak interactions between the sulfur atom of DPTS and the Cl radical.

3.2. Theoretical Kinetic Analysis. To gather more details about the rate of atmospheric degradation of DPTS with respect to Cl radicals, Master equation modeling of the various possible H-atom abstraction and substitution pathways (see Scheme 1) were performed using the Master equation solver for the multi-energy well reaction (MESMER v.5.2) code.[23] The detailed procedure for calculating the rate coefficients using Mesmer has been described previously in studies of the atmospheric oxidation of DMTS with OH/Cl radicals,[13] and DPTS with OH radicals,[11] and several other studies used the same code to study the kinetics of various atmospheric reactions.[34,36−39] The details associated with calculating the rate coefficients using Mesmer are also provided in this work. In computing the rate coefficients, Mesmer uses an energy-grained master equation approach in which the rotational−vibrational energy states for all the stationary points on the PES are divided into numerous energy grains, and each energy grain contains a defined number of energy states. The reactant (DPTS + $^{\bullet}$Cl) energy states were populated using a Boltzmann distribution, and the other minima on the PESs were set to a population of zero. The variation in population distribution between the energy states for all the minima on the PES can occur over the course of the reaction through the collisional energy transfer from one species to another, as well as via collision with a buffer gas.

3.2.1. Rate Coefficients. The results obtained from the present electronic structure calculations were used as input parameters in the Mesmer rate calculations. The input parameters used in Mesmer are zero-point-corrected CCSD(T)/M06-2X energies, vibrational frequencies, and rotational constants for all the key stationary points on the PESs for the possible H-abstraction and substitution paths (see Scheme 1) involved in the DPTS + $^{\bullet}$Cl reaction. The PESs, as shown in Figures 1, 3, and 4, indicate that the H-abstraction and substitution paths available to the DPTS + $^{\bullet}$Cl reaction involve three major forward reaction steps. First, association of the two reactants (DPTS and $^{\bullet}$Cl) occurs to form stable RCs, which can be seen at the entrance channels of each PESs. In the second step, the RCs undergo intramolecular isomerization, leading to the formation of PCs through a TS. In the third step, dissociation of the PC occurs to form final bimolecular products, which can also be seen at the exit channels of the PESs (see Figures 1, 3, and 4). The forward reactions of the entrance and reverse reactions of the exit channels for all the possible reaction paths occur on barrierless surfaces. Mesmer offers the choice of calculating the microcanonical rate coefficients [$k(E)$] for such barrierless reaction steps using the inverse Laplace transform method. This approach requires Arrhenius pre-exponential factors (A) for the entrance and exit channels of all possible H-abstraction and substitution paths. We used 1.85 × 10^{-11} and 1.00 × 10^{-11} cm^3 molecule^{-1} s^{-1} for the entrance and exit reaction steps of the H-atom abstraction paths, respectively. In the case of the substitution channels, Arrhenius pre-exponential factors (A) of 2.00 × 10^{-10} and 1.00 × 10^{-11} cm^3 molecule^{-1} s^{-1} for the entrance and exit channels, respectively, were used. These A values were taken from the experimentally measured rate coefficients reported for the H-abstraction and substitution paths involved in the $(CH_3)_2SO$ + $^{\bullet}$Cl and $(CH_3S)_2$ + $^{\bullet}$Cl reactions, respectively.[40,41] The aim of using these values was to ensure close agreement between the rate coefficients calculated using Mesmer, and the experimental values reported for the related analogous reactions: $(CH_3)_2SO$ + $^{\bullet}$Cl and $(CH_3S)_2$ + $^{\bullet}$Cl. The modified Arrhenius parameters and activation energies for the entrance and exit channels for all the H-abstraction and substitution paths were chosen to be 0.1 and 0 kcal mol^{-1}, respectively. The reaction step involving the conversion of RCs to PCs through a TS conforms to Rice−Ramsperger−Kassel−Marcus theory. The rate coefficient calculations included Eckart tunneling[42] corrections to account for potential tunneling contributions to the rate coefficients for all possible H-abstraction and substitution paths. Furthermore, Lennard-Jones (L-J) parameters (ε and σ) and a collision energy-transfer parameter $\langle\Delta E_d\rangle$ were also used in the present rate calculations. The depth of the potential well (ε), the finite length where the potential is zero (σ) for the RCs and PCs in all the PESs, and the bath gas were taken from previous reports. Briefly, nitrogen (N_2) bath gas was used in this work, with corresponding L-J parameters of σ = 3.9 Å and ε = 48 K.[23] The L-J parameters for the RCs and PCs were not available. Therefore, L-J parameters of n-nonane were used (i.e., σ = 6.56 Å and ε = 912.04 K)[43] as n-nonane and the RCs and PCs involving all possible paths are of similar size. We tested the sensitivity of the rate coefficients by monitoring the impact of using L-J parameters of both n-octane and n-decane. In these studies, we found no significant changes in the rate coefficients for all possible reaction paths. In addition, the collision energy transfer between intermediates and the bath gas was treated with a single-exponential collision energy-transfer model using an average collision energy-transfer value of $\langle\Delta E_d\rangle$ = 200 cm^{-1}. This value was chosen based on the literature-reported observations of Cl radical reactions with different atmospheric pollutants.[44,45]

https://doi.org/10.1021/acsearthspacechem.1c00246
ACS Earth Space Chem. 2021, 5, 2878−2890

The rate coefficients for all possible DPTS + •Cl elementary reactions were obtained by inputting the aforementioned parameters into the Mesmer code. The Master equation simulations utilize the Bartis−Widom method[46−49] to obtain phenomenological rate coefficients using the eigenvalues and eigenvectors of the system. The calculated rate coefficients (in cm^3 $molecule^{-1}$ s^{-1}) in the temperature range of 200−300 K and a pressure of 1 atm for all possible paths are displayed in Table S7. The results indicate that the rate coefficient values were almost independent of temperature for the reaction pathways proceeding through TS1a, TS1b, TS2b, TS5a, TS5b, TS6a, and TS6c in the studied temperatures between 200 and 300 K. For the reaction paths proceeding through TS2a, TS4a, TS4b, and TS6b, the rate coefficient values decreased with increasing temperature. On the other hand, for the reactions that proceeded via TS3a, TS3b, TS3c, TS7a, TS7b, TS8, and TS9, the rate coefficients were found to increase with temperature in the temperatures between 200 and 300 K. Overall, the rate coefficient values, as listed in Table S7, indicate that abstraction of H-atom by the Cl radical from the center carbon atom of the propyl group attached to the sulfinyl S-atom of DPTS, and which proceeds via TS2b, is ∼4.68×10^{-11} cm^3 $molecule^{-1}$ s^{-1} at 300 K, which is 5, 16, 8, 9, 22, and 15 times larger than the values of H-abstraction from the other possible sites via TS1a, TS1b, TS2a, TS3a, TS3b, and TS3c, respectively, at the same temperature. This large rate coefficient value for the abstraction reaction is mainly due to the lower barrier height that this reaction has compared to other possible H-abstraction paths. For the propyl group attached to the S-atom of DPTS, the Cl radical initiated abstraction of the H-atom linked to the $-CH_2$ group that is directly attached to the S-atom of DPTS, and which proceeds via TS4b, the rate coefficient was found to be ∼5.33×10^{-11} cm^3 $molecule^{-1}$ s^{-1} at 300 K, which is ∼8, 6, 1.5, 11, 13, and 18 times larger than the rate coefficient values for H-abstraction from the other possible sites of the same propyl group that proceed through TS4a, TS5a, TS5b, TS6a, TS6b, and TS6c, respectively, at the same temperature. Thus, for all possible H-abstraction paths for the DPTS + •Cl reaction, abstraction of the H-atom linked to the $-CH_2$ group that is attached directly to the S-atom of DPTS, and which proceeds through TS4b, is the most energetically feasible and therefore the most dominant process.

Rate coefficients were also calculated for the substitution channels in the temperatures between 200 and 300 K, and the values are reported in Table S7. The rate coefficient for the addition of the Cl radical to the sulfinyl group of DPTS via TS8 was calculated to be ∼6.00×10^{-10} cm^3 $molecule^{-1}$ s^{-1} at 300 K, which is ∼2−3 orders of magnitude larger than the rate coefficient values computed for the other substitution channels. Therefore, the present rate coefficient values for all possible abstraction and substitution paths indicate that addition of the Cl radical to the sulfinyl group of DPTS via TS8 to form propanesulfinyl chloride and PTR is kinetically more dominant, compared to all other possible DPTS + •Cl reaction paths.

The rate coefficients for the full range of possible DPTS + •Cl reaction paths were also calculated in the presence and absence of Eckart tunneling contributions, and the values are displayed in Tables S7 and S8 of the Supporting Information. The results displayed in these tables indicate that the tunneling contribution is significant for reactions that proceed via TS1b, TS3b, TS3c, TS6a, TS6b, TS6c, TS7a, and TS9 and that for the remaining paths, tunneling is insignificant in the entire studied temperature range. The rate coefficients for the reactions that occur via TS1b, TS3b, TS6a, TS6b, TS7a and TS9, were increased by 3, 2, 6, 2, 12, and 30 times in the studied temperature range when the tunneling parameter was included. For the reaction paths that proceed through TS3c and TS6c, tunneling resulted in rate coefficient increases of ∼2 times up to 250 K, beyond which tunneling contributions were found to be insignificant.

The overall rate coefficients (k_{total}) at each studied temperature were estimated by adding together all of the possible site-specific rate coefficients at each temperature, in the range between 200 and 300 K. The computed rate coefficient values were plotted (see Figure 5), and the values are listed in Table S7.

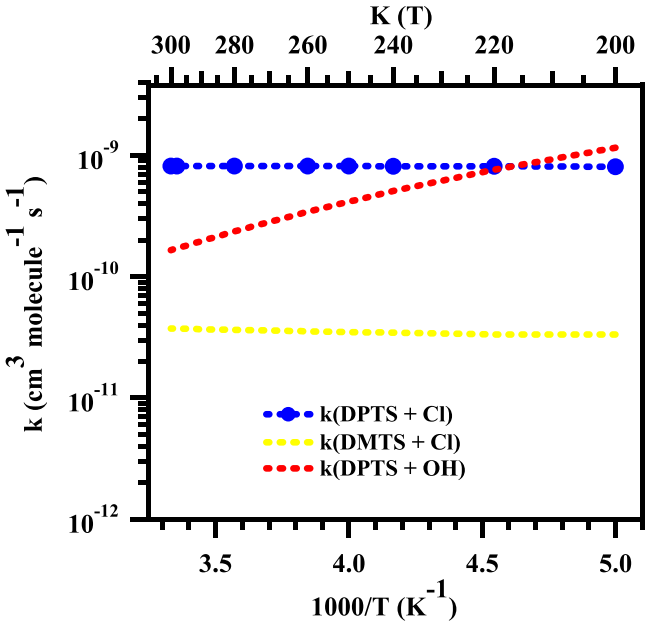

Figure 5. Comparison between the overall rate coefficients calculated for the DPTS + •Cl → products (blue dashed line) with that of the available overall rate coefficient values for the DPTS + •OH → products[11] (red dashed line) and DMTS + •Cl → products[13] (yellow dashed line) reactions in the temperatures between 200 and 300 K and at 760 Torr pressure. The overall rate coefficients represent the sum of all possible H-abstraction and substitution channel rate coefficients for the DPTS + •Cl, DPTS + •OH, and DMTS + •Cl reactions.

The results in Figure 5 and Table S7 show that the overall rate coefficients in the studied temperature range were almost independent of temperature. For example, the overall rate coefficient for the DPTS + •Cl reaction at 200 and 298 K were estimated to be 8.04×10^{-10} and 8.14×10^{-10} cm^3 $molecule^{-1}$ s^{-1}, respectively.

Experimentally measured and theoretically calculated rate coefficients for the DPTS + •Cl reaction were not available for comparison with the values calculated in this work. Therefore, we compared our calculated rate coefficient results with those of the analogous DMTS + •Cl and DPTS + •OH reactions, as shown in Figure 5. The rate coefficient values, as shown in Figure 5, for the DPTS + •Cl reaction calculated in this work are more than 1 order of magnitude larger than the values observed for the analogous DMTS + •Cl reaction in the temperatures between 200 and 300 K. For example, the overall rate coefficient computed here for the DPTS + •Cl reaction at 298 K was ∼22 times larger than that for the DMTS + •Cl reaction, which was reported to be 3.72×10^{-11} cm^3 $molecule^{-1}$ s^{-1} at the same temperature.[13] This difference in overall rate coefficients is mainly due to the presence of a greater number of H-abstraction

https://doi.org/10.1021/acsearthspacechem.1c00246
ACS Earth Space Chem. 2021, 5, 2878−2890

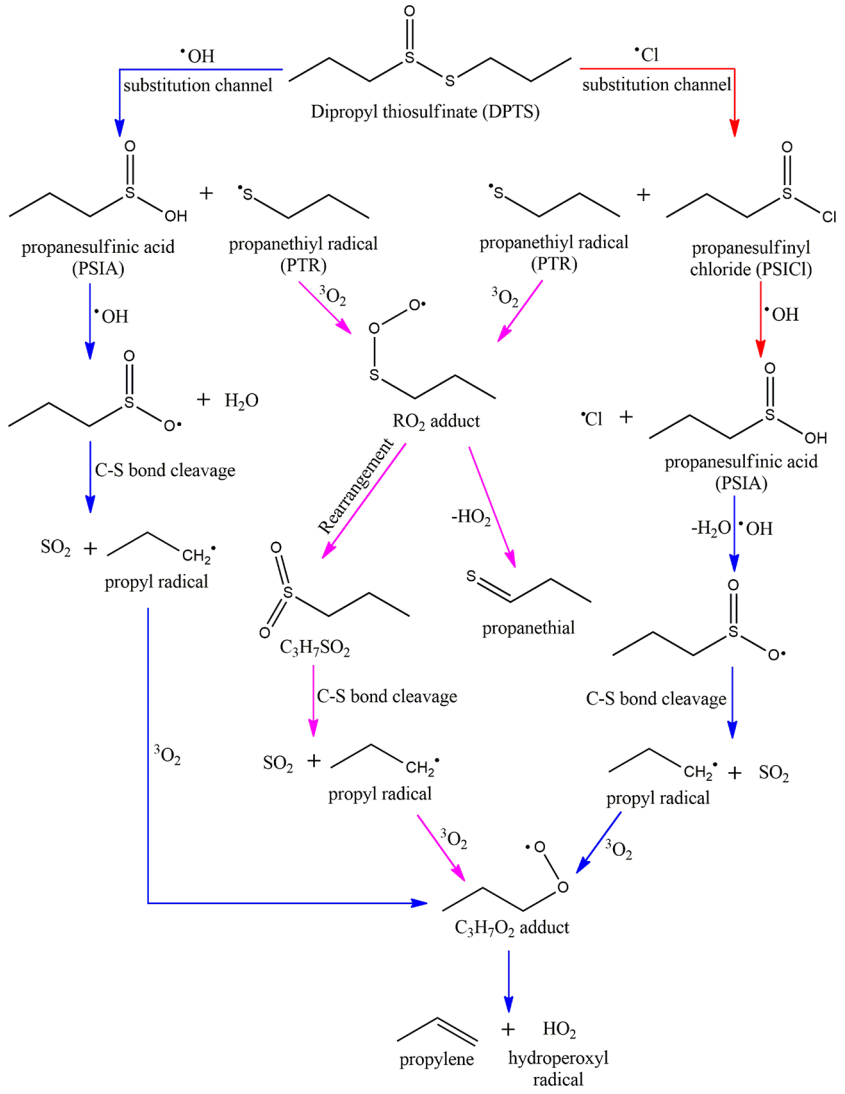

Figure 6. The most plausible degradation mechanism for DPTS in the presence of OH and Cl radicals under atmospherically relevant conditions. The mechanism of OH and Cl radical-initiated oxidation of DPTS to form various compounds is indicated by blue and red arrows, respectively. The reactions that occur when PTR is intercepted by atmospheric oxygen ($^3O_2$) are indicated with pink arrows.

sites in DPTS compared to DMTS. To better understand the relative reactivity of OH and Cl radicals with DPTS, we compared the rate coefficients of the DPTS + •Cl reaction with those of the DPTS + •OH reaction in the temperature range of 200−300 K. The results are also shown in Figure 5. The rate coefficient values, as shown in Figure 5, reveal that while they are larger above 220 K for the DPTS + •Cl reaction, they are smaller above this temperature when compared to the DPTS + •OH reaction. For example, the overall rate coefficient for the DPTS + •Cl reaction was estimated to be 8.14×10^{-10} cm^3 molecule^{-1} s^{-1} at 300 K, which is ∼5 times larger than that for the DPTS + •OH reaction, whose overall rate coefficient[11] was found to be 1.70×10^{-10} cm^3 molecule^{-1} s^{-1} at the same temperature. This suggests that when compared to the OH radical, Cl radical is more reactive for the removal of DPTS in the atmosphere.

To identify the relative contributions of each reaction path to the overall reaction in the temperatures between 200 and 300 K, branching ratio calculations were performed. The calculated results, presented as the percentage contribution of each of the elementary reaction paths (TS1a−TS9), are displayed in Table S9 of the Supporting Information. The branching ratio data, as listed in Table S9, suggest that the major contributor to the overall reaction is that which proceeds by Cl radical addition to the sulfinyl sulfur, followed by S(═O)−S bond fission through TS8, leading to the formation of PTR and propanesulfinyl chloride, with contributions from 72.2% to 73.6% between 200 and 300 K. The next highest branching contribution was the reaction involving H-abstraction via TS4b, with contributions from 6.8% at 200 K to 6.5% at 300 K. We observed an almost similar branching contribution from the H-abstraction path involving TS2b and TS5b, with contributions of 5.9% at 200 K to 5.8% at 300 K. The other remaining H-abstraction and substitution path contributions to the overall reaction were ∼1−3 orders of magnitude smaller compared to the values of the reaction that proceeded via TS8. We also estimated the contributions from the total abstraction and total substitution channels to the overall reaction in the studied temperature range. They were estimated to be ∼73.5% at 200 K to ∼75.0% at 300 K for the contributions from all substitution channels, with the remaining contributions from the abstraction paths being ∼26.5% at 200 K to 25.0% at 300 K.

https://doi.org/10.1021/acsearthspacechem.1c00246
ACS Earth Space Chem. 2021, 5, 2878−2890

3.3. Atmospheric Implications. DPTS is emitted from *Allium* genus cash crops, which occupy large acreage on farmlands throughout the world. Thus, it is important to understand the extent to which cultivated crops contribute to the environmental organosulfur burden through studies of the atmospheric fate of this and similar compounds and their oxidation products with atmospheric oxidants. This is particularly critical because several studies indicate that oxidation of VOSCs and their products in the atmosphere have significant effects on global warming, Earth's climate, human health, acid precipitation, and cloud formation.[9] The most plausible degradation mechanism proposed for the atmospheric removal of DPTS initiated by major atmospheric oxidants such as OH and Cl radicals is shown in Figure 6. This mechanism was derived based on dominant reactions obtained from the present work and considering the results of previous studies involving DPTS + OH radicals[11] and PSIA + $^{\bullet}$OH reactions.[39] The degradation mechanism suggests that DPTS primarily interacts with the atmospheric OH radical through a substitution channel by forming PSIA and PTR as products, as illustrated by the blue arrows in Figure 6. A recent study of the oxidation of PSIA initiated by the OH radical under atmospheric conditions suggests that the dominant path involves OH radical-initiated abstraction of the H-atom from the −OH moiety of PSIA, leading to the formation of the propanesulfinyl radical and water.[39] In the next step, the formed propanesulfinyl radical undergoes cleavage of the C−S single bond to form sulfur dioxide (SO_2) and propyl radicals as final products.

On the other hand, DPTS interacts with the Cl radical, another important atmospheric oxidant. The mechanism involving DPTS + Cl radicals is indicated by the red arrows in Figure 6. Similar to the DPTS + OH radical reaction, the Cl radical also interacts with DPTS through a substitution channel to form propanesulfinyl chloride (PSICl) and PTR as products. Furthermore, the formed PSICl can interact with the OH radical at the S-atom of the sulfinyl [−S(=O)] group followed by simultaneous cleavage of the S−Cl single bond, leading to the formation of PSIA and Cl radical as products (see Figure 6). This suggests that the formed PSICl acts as a potential source for Cl radicals. Furthermore, the generated PSIA proceeds to form propanesulfinyl radical + H_2O and eventually to SO_2 and propyl radical, as indicated by the blue arrows in Figure 6. In addition, DPTS + OH/Cl radical reactions produce PTR as a common product. The fate of PTR under atmospheric conditions was reported in previous work[11] to involve reaction with atmospheric oxygen ($^3O_2$), leading to the corresponding RO_2 adduct, where (R = $CH_3CH_2CH_2S-$). The RO_2 adduct undergoes decomposition through HO_2 elimination to form propanethial and intramolecular rearrangement to form $C_3H_7SO_2$ as a product, which then undergoes C−S single bond cleavage to form SO_2 and propyl radicals (as indicated by the pink arrows). It was also suggested that the elimination of the HO_2 radical to form propanethial is dominant when concentrations of NO are low.[11] Finally, the formed propyl radicals are expected to undergo rapid reaction with $^3O_2$ to form $C_3H_7O_2$ radicals, which then undergo unimolecular elimination to form propylene and HO_2 radicals as major products (as indicated by the blue arrows).

The cumulative atmospheric lifetime of DPTS with respect to its reactions with OH and Cl radicals was calculated using eq 1.[50−52]

$$\frac{1}{\tau_{\text{eff}}} = \frac{1}{\tau_{\text{OH}}} + \frac{1}{\tau_{\text{Cl}}} \quad (1)$$

In eq 1, the term τ_{eff} represents the cumulative lifetime of DPTS. The other terms τ_{OH} and τ_{Cl} represent the atmospheric lifetimes of DPTS with respect to its reactions with OH and Cl radicals, respectively. The lifetime (τ) of any atmospheric molecule can be calculated using the equation[50−52] $\tau = 1/k[X]$, where "k" represents the bimolecular rate coefficients for the DPTS + $^{\bullet}$Cl or DPTS + $^{\bullet}$OH reaction, and "[X]" represents the OH or Cl radical concentration. The average atmospheric concentrations of [$^{\bullet}$OH] = 1.0×10^6 molecules cm^{-3} and [$^{\bullet}$Cl] = 1.3×10^5 atoms cm^{-3}, respectively,[14,15,53] were used in calculating the atmospheric lifetime of DPTS with the corresponding $^{\bullet}$OH and $^{\bullet}$Cl radicals. The bimolecular rate coefficient for the DPTS + $^{\bullet}$Cl reaction was taken from this work and that for the DPTS + $^{\bullet}$OH reaction was taken from the literature.[11] The atmospheric lifetimes for DPTS, which are presented in Table 1, were computed to be ∼2.6 h with respect to its reaction with the Cl radical and ∼1.7 h with respect to its reaction with the OH radical. Because the OH radical concentration in the atmosphere is ∼10 times larger than the Cl radical concentration, the atmospheric removal of DPTS occurs mostly via its reaction with OH radicals, even though the DPTS + $^{\bullet}$Cl reaction rate coefficient at 300 K is ∼5 times larger than that for the DPTS + $^{\bullet}$OH reaction (see Table 1). The cumulative lifetime (τ_{eff}) of DPTS in its reactions with OH and Cl radicals was calculated to be only ∼1.02 h. This reveals that the DPTS contribution to global warming is negligible. However, DPTS emissions from plants into the atmosphere still have the potential to contribute to global warming and formation of aerosols through their oxidative decomposition to form sulfur dioxide (SO_2), HCl, propanesulfinyl chloride ($CH_3CH_2CH_2S(O)Cl$), propanethial, and HO_2 radical. In addition, minor substitution paths of the DPTS + $^{\bullet}$Cl reaction may produce small amounts of chlorinated products such as $CH_3CH_2CH_2SCl$ and $CH_3CH_2CH_2SS(O)Cl$ along with the major product (propanesulfinyl chloride) released into the atmosphere. These chlorinated compounds might have adverse effects on the stratospheric ozone layer.

Table 1. Atmospheric Lifetimes (τ) Calculated for the Reactions of DPTS with $^{\bullet}$OH and $^{\bullet}$Cl Radicals at 300 K

reaction	k (cm^3 molecule^{-1} s^{-1})	τ (h)[c]
DPTS + $^{\bullet}$Cl → products[a]	8.14×10^{-10}	2.62
DPTS + $^{\bullet}$OH → products[b]	1.70×10^{-10}	1.69
cumulative lifetime (τ_{eff})		1.02

[a]Present work. [b]Arathala and Musah.[11] [c]Concentrations of [OH] = 1.0×10^6 molecules cm^{-3} and [Cl] = 1.3×10^5 atoms cm^{-3} were used in calculating the atmospheric lifetime of DPTS at 300 K.

In the marine boundary layer, the concentration of Cl radicals is estimated to be 1−10% of the concentration of OH radicals. Using these concentration ranges, the atmospheric removal of DPTS due to its reactions with the Cl radical can be estimated using the formula $k_{Cl}[Cl]/k_{OH}[OH]$. The contribution of Cl radicals to the removal of DPTS was calculated to be 5−60% compared to the contribution of the $^{\bullet}$OH radical reaction at 298 K. The tropospheric lifetime of DPTS with respect to its reaction with $^{\bullet}$OH was calculated to be 1.7 h, which changed to 1.0 h when considered from the perspective of both OH and Cl radicals. Therefore, the tropospheric lifetime of DPTS will be

https://doi.org/10.1021/acsearthspacechem.1c00246
ACS Earth Space Chem. 2021, 5, 2878−2890

overestimated by ∼70% if the role of •Cl in the atmospheric removal of DPTS is ignored, especially when the huge area of the oceans and the continental urban areas are considered. This further illustrates the importance of Cl radical reactions in the removal of DPTS in the troposphere.

In addition, the nitrate (NO_3) radical is an important nighttime oxidant for the degradation of organic compounds. Numerous reports on the atmospheric oxidation of DMSO [$CH_3S(O)CH_3$] and divinyl sulfoxide [CH_2═$CHS(O)CH$═CH_2] with NO_3 radical have appeared.[8,54,55] These studies indicate that the reactions with NO_3 radicals play a significant role in the degradation of organosulfur compounds in the troposphere. Therefore, reactions with NO_3 may also be expected to be important transformation processes for DPTS in the troposphere. The DPTS + NO_3 radical reaction path may proceed via H-abstraction by NO_3 from C−H bonds to form C-centered DPTS radical products and molecular nitric acid (HNO_3). It is also possible that the NO_3 radical adds to the sulfinyl group and S-atom of DPTS followed by S(═O)−S and S(═O)−C single bond cleavage to form various products. In addition, the reaction of the atmospheric ClO radical with DPTS may be useful in further understanding the reactivity of these radicals with VOSCs in determining the composition of Earth's atmosphere. Similar to the DPTS + NO_3 radical reaction, DPTS + ClO radical reactions may also proceed via H-abstraction by ClO radicals and its addition to the sulfinyl group and S-atom followed by S(═O)−S and S(═O)−C single bond cleavage to form various products. Further studies are required to get a more complete portrait of the mechanism and degradation products involving oxidation of DPTS with NO_3 and ClO radicals under normal atmospheric conditions.

4. CONCLUSIONS

The atmospheric oxidation mechanism of DPTS via its reaction with the Cl radical was investigated at the CCS(D)T/cc-pVTZ//M06-2X/aug-cc-pVTZ level. The kinetics of all the H-atom abstraction and substitution pathways were calculated using the Mesmer kinetic code over a temperature range of 200−300 K and at 1 atm pressure. From the analysis of the above results, the following conclusions have been drawn:

(i) The addition of the Cl radical to the S-atom of the sulfinyl moiety, followed by S(═O)−S single bond cleavage, leading to the formation of PTR and propanesulfinyl chloride is the major reaction path.

(ii) The calculated branching ratios indicate that formation of propanesulfinyl chloride and PTR from the DPTS + •Cl reaction contributes ∼74% to the overall reaction at 298 K and 1 atm.

(iii) The atmospheric lifetime of DPTS with respect to the Cl radical was estimated to be ∼2.6 h in the temperature range between 200 and 300 K and at 1 atm pressure.

(iv) The most plausible atmospheric oxidation mechanism for DPTS with OH and Cl radicals suggests that these reactions generate mainly sulfur dioxide (SO_2), propylene, hydroperoxyl (HO_2) radical, propanethial, Cl radical, and water.

(v) The cumulative lifetime of DPTS with respect to its reaction with OH and Cl radicals was found to be 1 h. This suggests that this compound rapidly decomposes in the troposphere and exhibits a negligible impact on global warming. However, the major products formed (i.e., SO_2, HCl, propanesulfinyl chloride, propanethial, and HO_2 radical), and minor chlorinated products which include $CH_3CH_2CH_2SCl$ and $CH_3CH_2CH_2SS(O)Cl$, may make significant contributions to the formation of SOA and acid rain and may have adverse effects on global warming and the ozone layer.

■ ASSOCIATED CONTENT

Supporting Information

The Supporting Information is available free of charge at https://pubs.acs.org/doi/10.1021/acsearthspacechem.1c00246.

T1 diagnostic values, calculated total electronic energies including ZPE corrections, imaginary frequencies of various TSs at the M06-2X level, optimized geometries of all the stationary points, their vibrational frequencies, rotational constants, bimolecular rate coefficients in the absence and presence of tunneling contributions for each reaction path, and the optimized geometries of RCs and PCs associated with the DPTS + •Cl reaction (PDF)

■ AUTHOR INFORMATION

Corresponding Author

Rabi A. Musah − *Department of Chemistry, University at Albany—State University of New York, Albany, New York 12222, United States;* orcid.org/0000-0002-3135-4130; Email: rmusah@albany.edu

Author

Parandaman Arathala − *Department of Chemistry, University at Albany—State University of New York, Albany, New York 12222, United States*

Complete contact information is available at: https://pubs.acs.org/10.1021/acsearthspacechem.1c00246

Notes

The authors declare no competing financial interest.

■ ACKNOWLEDGMENTS

Financial support of the National Science Foundation (grant numbers 1310350 and 1710221) to R.A.M. is gratefully acknowledged. The authors also thank the High-Performance Computing Center at the University at Albany-SUNY for its support.

■ REFERENCES

(1) Graedel, T. E. Reduced sulfur emission from the open oceans. *Geophys. Res. Lett.* **1979**, *6*, 329−331.

(2) Aneja, V. P.; Cooper, W. J. Biogenic Sulfur Emissions. In *Biogenic Sulfur in the Environment*, American Chemical Society: 1989; Vol. *393*, pp 2-13. DOI: 10.1021/bk-1989-0393.ch001

(3) Wine, P. H.; Thompson, R. J.; Semmes, D. H. Kinetics of OH reactions with aliphatic thiols. *Int. J. Chem. Kinet.* **1984**, *16*, 1623−1636.

(4) Mai, T. V.-T.; Nguyen, H. T.; Huynh, L. K. Kinetics of hydrogen abstraction from CH_3SH by OH radicals: An ab initio RRKM-based master equation study. *Atmos. Environ.* **2020**, *242*, 117833.

(5) Kleissas, K. M.; Nicovich, J. M.; Wine, P. H. Spectroscopy and kinetics of the gas phase addition complex of atomic chlorine with dimethyl sulfoxide. *J. Photochem. Photobiol., A* **2007**, *187*, 1−9.

(6) Asatryan, R.; Bozzelli, J. W. Formation of a Criegee intermediate in the low-temperature oxidation of dimethyl sulfoxide. *Phys. Chem. Chem. Phys.* **2008**, *10*, 1769−1780.

(7) Lv, G.; Zhang, C.; Sun, X. Understanding the oxidation mechanism of methanesulfinic acid by ozone in the atmosphere. *Sci. Rep.* **2019**, *9*, 322.
(8) Falbe-Hansen, H.; Sørensen, S.; Jensen, N. R.; Pedersen, T.; Hjorth, J. Atmospheric gas-phase reactions of dimethylsulphoxide and dimethylsulphone with OH and NO_3 radicals, Cl atoms and ozone. *Atmos. Environ.* **2000**, *34*, 1543−1551.
(9) Bentley, R.; Chasteen, T. G. Environmental VOSCs–formation and degradation of dimethyl sulfide, methanethiol and related materials. *Chemosphere* **2004**, *55*, 291−317.
(10) Block, E.; Putman, D.; Zhao, S. H. Allium chemistry: GC-MS analysis of thiosulfinates and related compounds from onion, leek, scallion, shallot, chive, and Chinese chive. *J. Agric. Food Chem.* **1992**, *40*, 2431−2438.
(11) Arathala, P.; Musah, R. A. Computational study investigating the atmospheric oxidation mechanism and kinetics of dipropyl thiosulfinate initiated by OH radicals and the fate of propanethiyl radical. *J. Phys. Chem. A* **2020**, *124*, 8292−8304.
(12) Gligorovski, S.; Strekowski, R.; Barbati, S.; Vione, D. Environmental Implications of Hydroxyl Radicals (OH). *Chem. Rev.* **2015**, *115*, 13051−13092.
(13) Arathala, P.; Musah, R. A. Theoretical studies of the gas-phase reactions of s-methyl methanesulfinothioate (dimethyl thiosulfinate) with OH and Cl radicals: Reaction mechanisms, energetics, and kinetics. *J. Phys. Chem. A* **2019**, *123*, 8448−8459.
(14) Spicer, C. W.; Chapman, E. G.; Finlayson-Pitts, B. J.; Plastridge, R. A.; Hubbe, J. M.; Fast, J. D.; Berkowitz, C. M. Unexpectedly high concentrations of molecular chlorine in coastal air. *Nature* **1998**, *394*, 353−356.
(15) Singh, H. B.; Thakur, A. N.; Chen, Y. E.; Kanakidou, M. Tetrachloroethylene as an indicator of low Cl atom concentrations in the troposphere. *Geophys. Res. Lett.* **1996**, *23*, 1529−1532.
(16) Wingenter, O. W.; Kubo, M. K.; Blake, N. J.; Smith, T. W., Jr.; Blake, D. R.; Rowland, F. S. Hydrocarbon and halocarbon measurements as photochemical and dynamical indicators of atmospheric hydroxyl, atomic chlorine, and vertical mixing obtained during Lagrangian flights. *J. Geophys. Res.* **1996**, *101*, 4331−4340.
(17) Barone, S. B.; Turnipseed, A. A.; Ravishankara, A. R. Role of adducts in the atmospheric oxidation of dimethyl sulfide. *Faraday Discuss.* **1995**, *100*, 39−54.
(18) Williams, M. B.; Campuzano-Jost, P.; Cossairt, B. M.; Hynes, A. J.; Pounds, A. J. Experimental and Theoretical Studies of the Reaction of the OH Radical with Alkyl Sulfides: 1. Direct Observations of the Formation of the OH−DMS Adduct−Pressure Dependence of the Forward Rate of Addition and Development of a Predictive Expression at Low Temperature. *J. Phys. Chem. A* **2007**, *111*, 89−104.
(19) Urbanski, S. P.; Wine, P. H. Spectroscopic and kinetic study of the Cl−S$(CH_3)_2$ adduct. *J. Phys. Chem. A* **1999**, *103*, 10935−10944.
(20) Nicovich, J. M.; Parthasarathy, S.; Pope, F. D.; Pegus, A. T.; McKee, M. L.; Wine, P. H. Kinetics, Mechanism, and Thermochemistry of the Gas Phase Reaction of Atomic Chlorine with Dimethyl Sulfoxide. *J. Phys. Chem. A* **2006**, *110*, 6874−6885.
(21) Resende, S. M.; De Almeida, W. B. Theoretical study of the atmospheric reaction between dimethyl sulfide and chlorine atoms. *J. Phys. Chem. A* **1997**, *101*, 9738−9744.
(22) Uchimaru, T.; Tsuzuki, S.; Sugie, M.; Tokuhashi, K.; Sekiya, A. A theoretical study on the strength of two-center three-electron bond in $(CH_3)_2S$−OH and H_2S−OH adducts. *Chem. Phys. Lett.* **2005**, *408*, 216−220.
(23) Glowacki, D. R.; Liang, C.-H.; Morley, C.; Pilling, M. J.; Robertson, S. H. MESMER: an open-source master equation solver for multi-energy well reactions. *J. Phys. Chem. A* **2012**, *116*, 9545−9560.
(24) Zhao, Y.; Truhlar, D. G. The M06 suite of density functionals for main group thermochemistry, thermochemical kinetics, noncovalent interactions, excited states, and transition elements: two new functionals and systematic testing of four M06-class functionals and 12 other functionals. *Theor. Chem. Acc.* **2008**, *120*, 215−241.
(25) Kendall, R. A.; Dunning, T. H., Jr.; Harrison, R. J. Electron affinities of the first-row atoms revisited. Systematic basis sets and wave functions. *J. Chem. Phys.* **1992**, *96*, 6796−6806.
(26) Arathala, P.; Katz, M.; Musah, R. A. Reaction mechanism, energetics, and kinetics of the water-assisted thioformaldehyde + $\dot{O}H$ reaction and the fate of its product radical under tropospheric conditions. *Phys. Chem. Chem. Phys.* **2020**, *22*, 10027−10042.
(27) Fukui, K. The path of chemical reactions—the IRC approach. *Acc. Chem. Res.* **1981**, *14*, 363−368.
(28) Hratchian, H. P.; Schlegel, H. B. Chapter 10—Finding minima, transition states, and following reaction pathways on ab Initio potential energy surfaces. In *Theory and Applications of Computational Chemistry*; Dykstra, C. E., Frenking, G., Kim, K. S., Scuseria, G. E., Eds.; Elsevier: Amsterdam, 2005; pp 195−249.
(29) Noga, J.; Bartlett, R. J. The full CCSDT model for molecular electronic structure. *J. Chem. Phys.* **1987**, *86*, 7041−7050.
(30) Frisch, M. J.; Trucks, G. W.; Schlegel, H. B.; Scuseria, G. E.; Robb, M. A.; Cheeseman, J. R.; Scalmani, G.; Barone, V.; Petersson, G. A.; Nakatsuji, H.; et al. *Gaussian 16*, Revision B.01; Gaussian, Inc.: Wallingford, CT, 2016.
(31) Lee, T. J.; Taylor, P. R. A diagnostic for determining the quality of single-reference electron correlation methods. *Int. J. Quantum Chem., Symp.* **1989**, *36*, 199−207.
(32) Zhu, L.; Nicovich, J. M.; Wine, P. H. Kinetics studies of aqueous phase reactions of Cl atoms and Cl_2- radicals with organic sulfur compounds of atmospheric interest. *J. Phys. Chem. A* **2005**, *109*, 3903−3911.
(33) Kishore, K.; Asmus, K. D. Nature of $2\sigma/1\sigma^*$ three-electron-bonded chlorine adducts to sulfoxides. *J. Phys. Chem.* **1991**, *95*, 7233−7239.
(34) Nicovich, J. M.; Mazumder, S.; Laine, P. L.; Wine, P. H.; Tang, Y.; Bunkan, A. J. C.; Nielsen, C. J. An experimental and theoretical study of the gas phase kinetics of atomic chlorine reactions with CH_3NH_2, $(CH_3)_2NH$, and $(CH_3)_3N$. *Phys. Chem. Chem. Phys.* **2015**, *17*, 911−917.
(35) Xie, H.-B.; Ma, F.; Yu, Q.; He, N.; Chen, J. Computational Study of the Reactions of Chlorine Radicals with Atmospheric Organic Compounds Featuring NHx-π-Bond (x = 1, 2) Structures. *J. Phys. Chem. A* **2017**, *121*, 1657−1665.
(36) Parandaman, A.; Kumar, M.; Francisco, J. S.; Sinha, A. Organic acid formation from the atmospheric oxidation of gem diols: Reaction mechanism, energetics, and rates. *J. Phys. Chem. A* **2018**, *122*, 6266−6276.
(37) Zhao, X.; Wang, L. Atmospheric oxidation mechanism of furfural initiated by hydroxyl radicals. *J. Phys. Chem. A* **2017**, *121*, 3247−3253.
(38) Carr, S. A.; Still, T. J.; Blitz, M. A.; Eskola, A. J.; Pilling, M. J.; Seakins, P. W.; Shannon, R. J.; Wang, B.; Robertson, S. H. Experimental and theoretical study of the kinetics and mechanism of the reaction of OH radicals with dimethyl ether. *J. Phys. Chem. A* **2013**, *117*, 11142−11154.
(39) Arathala, P.; Musah, R. A. Atmospheric oxidation of propanesulfinic acid initiated by OH radicals: Reaction mechanism, energetics, rate coefficients, and atmospheric implications. *ACS Earth Space Chem.* **2021**, *5*, 1498−1510.
(40) Kambanis, K. G.; Lazarou, Y. G.; Papagiannakopoulos, P. Kinetic studies of the reaction of Cl atoms with CH_3SSCH_3. *J. Chem. Soc., Faraday Trans.* **1996**, *92*, 4905−4908.
(41) Riffault, V.; Bedjanian, Y.; Le Bras, G. Kinetic and mechanistic study of the X and XO (X = Cl, Br) reactions with dimethyl sulfoxide. *Phys. Chem. Chem. Phys.* **2003**, *5*, 2828−2835.
(42) Miller, W. H. Tunneling corrections to unimolecular rate constants, with application to formaldehyde. *J. Am. Chem. Soc.* **1979**, *101*, 6810−6814.
(43) Sun, T.; Teja, A. S. An equation of state for real fluids based on the lennard-jones potential. *J. Phys. Chem.* **1996**, *100*, 17365−17372.
(44) Xie, H.-B.; Ma, F.; Wang, Y.; He, N.; Yu, Q.; Chen, J. Quantum chemical study on ·Cl-initiated atmospheric degradation of monoethanolamine. *Environ. Sci. Technol.* **2015**, *49*, 13246−13255.

https://doi.org/10.1021/acsearthspacechem.1c00246
ACS Earth Space Chem. 2021, 5, 2878−2890

(45) Ma, F.; Ding, Z.; Elm, J.; Xie, H.-B.; Yu, Q.; Liu, C.; Li, C.; Fu, Z.; Zhang, L.; Chen, J. Atmospheric oxidation of piperazine initiated by · Cl: Unexpected high nitrosamine yield. *Environ. Sci. Technol.* **2018**, *52*, 9801−9809.
(46) Bartis, J. T.; Widom, B. Stochastic models of the interconversion of three or more chemical species. *J. Chem. Phys.* **1974**, *60*, 3474−3482.
(47) Miller, J. A.; Klippenstein, S. J. Master equation methods in gas phase chemical kinetics. *J. Phys. Chem. A* **2006**, *110*, 10528−10544.
(48) Miller, J. A.; Klippenstein, S. J.; Robertson, S. H.; Pilling, M. J.; Green, N. J. B. Detailed balance in multiple-well chemical reactions. *Phys. Chem. Chem. Phys.* **2009**, *11*, 1128−1137.
(49) Robertson, S. H.; Pilling, M. J.; Jitariu, L. C.; Hillier, I. H. Master equation methods for multiple well systems: application to the 1-,2-pentyl system. *Phys. Chem. Chem. Phys.* **2007**, *9*, 4085−4097.
(50) Kurylo, M. J.; Orkin, V. L. Determination of atmospheric lifetimes via the measurement of OH radical kinetics. *Chem. Rev.* **2003**, *103*, 5049−5076.
(51) Papadimitriou, V. C.; Kambanis, K. G.; Lazarou, Y. G.; Papagiannakopoulos, P. Kinetic study for the reactions of several hydrofluoroethers with chlorine atoms. *J. Phys. Chem. A* **2004**, *108*, 2666−2674.
(52) Mishra, B. K.; Lily, M.; Deka, R. C.; Chandra, A. K. A theoretical insight into atmospheric chemistry of HFE-7100 and perfluoro-butyl formate: reactions with OH radicals and Cl atoms and the fate of alkoxy radicals. *New J. Chem.* **2016**, *40*, 6148−6155.
(53) Atkinson, R. Atmospheric chemistry of VOCs and NOx. *Atmos. Environ.* **2000**, *34*, 2063−2101.
(54) Aschmann, S. M.; Tuazon, E. C.; Long, W. D.; Atkinson, R. Kinetics and products of the gas-phase reactions of divinyl sulfoxide with OH and NO_3 radicals and O_3. *J. Phys. Chem. A* **2008**, *112*, 8723−8730.
(55) Barnes, I.; Hjorth, J.; Mihalopoulos, N. Dimethyl sulfide and dimethyl sulfoxide and their oxidation in the atmosphere. *Chem. Rev.* **2006**, *106*, 940−975.

https://doi.org/10.1021/acsearthspacechem.1c00246
ACS Earth Space Chem. 2021, 5, 2878−2890